Asian Journal of Chemistry; Vol. 30, No. 7 (2018), 1617-1620

ASIAN JOURNAL OF CHEMISTRY

https://doi.org/10.14233/ajchem.2018.21280

Colloidal Co-Crystallization: A New Route for Production of Three-Dimensional Metallodielectric Photonic Crystals

SYARA KASSIM[1,*] and MARTYN PEMBLE[2,3]

[1]Advanced Nano Materials Research Group, School of Fundamental Science, Universiti Malaysia Terengganu, 21030 Kuala Terengganu, Terengganu, Malaysia
[2]Department of Chemistry, University College Cork, College Road, Cork, Ireland
[3]Tyndall National Institute, University College Cork, Dyke Parade, Cork, Ireland

*Corresponding author: Tel: + 60 9 6883165; E-mail: syara.kassim@umt.edu.my

Received: 13 February 2018; *Accepted*: 26 March 2018; *Published online*: 31 May 2018; AJC-18942

Growth of three-dimensional (3D) photonic crystals is most interesting research in new and enhancing devices performance ranging from sensor, optoelectronic, photovoltaic and also surface enhance Raman scattering. Co-crystallization with bottom up technique was introduced in producing 3D photonic crystals with metal properties or so called as metallodielectric photonic crystals and also its inverse structure. In this study, poly(methyl methacrylate) (PMMA) particles, acid-hydrolyzed tetraethylorthosilicate solution and pre-formed gold nanoparticles was combined followed by the removal of PMMA template. Relatively large (10 s of mm), robust and crack-free films with thickness of approximately below 20 deposition layers was successfully produced by this simple yet effective route. Its morphology, particle size and optical properties were characterized by scanning electron microscopy (SEM), optical bench set-up.

Keywords: Photonic crystals, Poly(methyl methacrylate), Colloids, Nanostructured polymers, Optical Properties, Films.

INTRODUCTION

Photonic crystals are periodic dielectric structure that arrange in periodic fashion to form a crystals. As a one class of functional materials with periodically in dielectric constant where the ability of this structure to manipulate light either forbids and transmit photonic crystals appears to be major concern among researchers for several applications from full-colour displays, paints and photonic paper until the potentiality to be exploits for improvement of technology and devices. The idea of blending photonic with plasmonic properties of metal such as gold and silver nanoparticles could integrated plasmonic-photonic materials stem for elevated novel optical functionalities that could be recognize from the fundamental optical interactions between photonic band gaps and the localized surface plasmon resonance in the photonic crystals, which does not occur in natural or bulk system [1]. Since, the partage of properties in one material, this structure was called metallodielectric photonic crystals. The propagation of light inside the materials is well-linked with the response of its optical impulse. The interaction between this optical field and electromagnetic waves resulting in novel quantum optical phenomena that significant to important technological applications such as zero threshold microlaser, single mode LED and optical transistor [2-4]. The practice of using colloidal crystal matrix are being suggested which consist of random distribution of gold nanoparticles which can be efficient mode toward inspecting the component of optical properties of 3D metallodielectric photonic crystals (MDPC). The approach of using poly(methyl methacrylate) (PMMA) beads as one of the colloidal for co-crystallize with silica is due to its non-toxic preparation and used as template as can be removed easily for further inverted structure. The presence of silica promising thin film with minimum cracking as silica act as cementing agent where also capable to hold metal nanoparticles in the matrix.

One of the ways that can be used to reduce the expenditure for the making of sub-micrometer 3D photonic crystals are called as bottom up colloidal crystallization [5-8]. In comparing several technique that enable preliminary verification of the exclusive optical properties of MDPC thin film ranging from chemical infiltration [8], atomic layer deposition (ALD) [9], chemical vapour deposition (CVD) [10] and electrodeposition [11]. However, self -assembly with controlled evaporation was selected in fabricating 3D MPDC thin film in this study since some of the technique may contribute in producing highly packed arrangement with void exception where may distinguished the properties of band gap.

Co-crystallization of PMMA, silica with gold nanoparticles and also the silica/gold inverse opal thin film was successfully obtained and fabricated by using bottom up technique in this study. The morphology and optical properties of these thin films

was conducted by using scanning electron microscopy (SEM), transmission electron microscopy (TEM) and optical bench top. The performance of this 3D MDPC and inverse MDPC promising great deal towards low cost photovoltaic application which role as energy harvesting and trapping modules.

EXPERIMENTAL

Methyl methacrylate monomer (MMA, 99%), polyethyleneimine (PEI, 80%), poly(styrene-4-sulphonate) (PSS), tetraorthosilicate (TeOS) and gold(III) chloride trihydrate were purchased from Aldrich (Milwaukee, USA) while, acetone, hydrochloric acid, sodium borohydride, trisodium citrate, ammonia hydroxide were purchased from R&M Marketing (U.K.). Hydrogen peroxide and ethanol (95%) was purchased from HmbG, Germany. Deionized water (resistivity 18.0 MΩ) was used for the preparation of all solutions. All chemicals and solvent were used as received without further purification. Reactions were carried out in the fume hood.

Preparation of silica/gold inverse opal: The PMMA spheres with about 373 nm size were synthesized *via* surfactant free emulsion polymerization as described earlier [1]. The gold nanoparticles were prepared by $NaBH_4$ reduction with citrate stabilized. Tetraorthosilicate solution precursor was prepared with a ratio of 8:1:1 to ethanol and HCl (0.1 M). For the fabrication purpose, clean and treated glass substrate were used. The glass substrate were cleaned and treated with mixture of water, ammonium hydroxide and H_2O_2 with volume ratio 5:1:1, respectively for 2 h while shaking. Instead of cleaning the glass surface from any matter, this step was also believed in increasing the hydrophobicity of the surface for colloidal patched.

Inverted structure of MPDC thin film was initially grew by vertical deposition with highly controlled evaporation from suspension of mixture PMMA, TeOS and silver nanoparticles. The resulted assemble thin film was continued with the removal of PMMA to form an inverted opal structure on the glass substrate by soaking in acetone and undergoing calcination process at 350-400 ºC. The inverted structure without silver nanoparticles also was fabricated to compare with inverted MPDC [12]. All of the resulting thin film was further characterized by using scanning electron microscopy (SEM), transmission electron microscopy (TEM) and table set-up optic in order to obtaining the morphology, size and optical properties for its potential applications.

RESULTS AND DISCUSSION

Size and morphology: Fig. 1 (SEM) shows the morphology for co-crystallization of TeOS-PMMA thin film and the inverted structure. From the image obvious inverted skeleton could be observed with highly periodic arranged and wide area consistently covered. The presence of TeOS as cementing agent able to hold gold nanoparticles in photonic crystals skeleton while producing less cracking thin film for opal and inverted opal structure.

From the excellent photonic crystals skeleton formation, the idea of inclusion metallic silver nanoparticles was introduced in order to explore the combination of unique properties of photonic and surface plasmon resonance. Fig. 2 shows morphology of inverted MPDC structure where the scattered of gold nanoparticles can clearly be observed embedded in photonic crystals skeleton.

Optical properties: Inverse Opal and inverse MPDC was investigated its optical properties by using an optical bench set-up at 450 to 1100 nm as demonstrated in Fig. 3. From the graph, the Bragg peak shift was observed together with the expansion in refractive index compared upon contradict for both PMMA opal and the inverted structure with silica.

Fig. 4 shows the graph of transmission and reflectance for inverted MPDC structure with two difference percentages of gold nanoparticles incorporated. From the graph, there is obvious red shifted of the wavelength from 749 to 779 nm when the gold nanoparticles preoccupation was increase. For comparison purpose reflectance and transmission spectra of PMMA

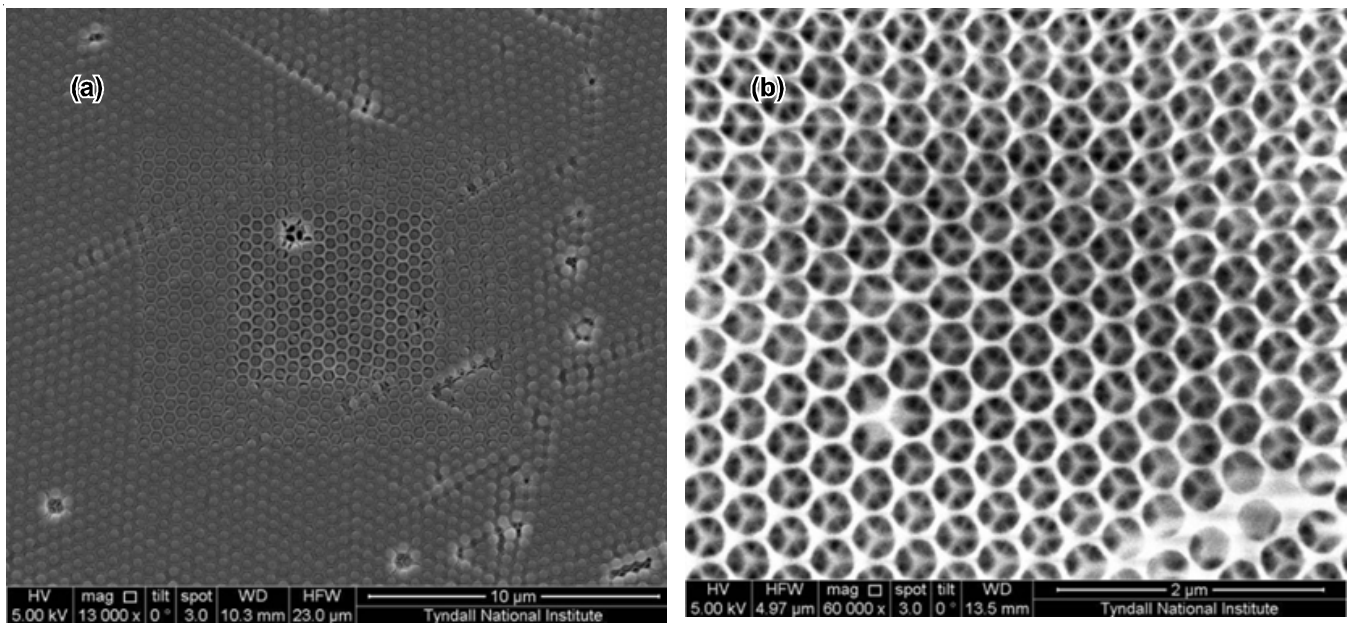

Fig. 1. SEM image for (a) co-crystallize thin film and (b) inverted structure thin film

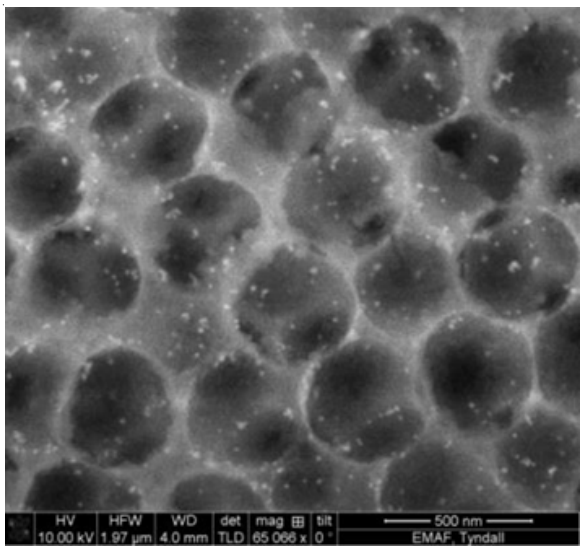

Fig. 2. TEM image of MPDC inverted skeleton

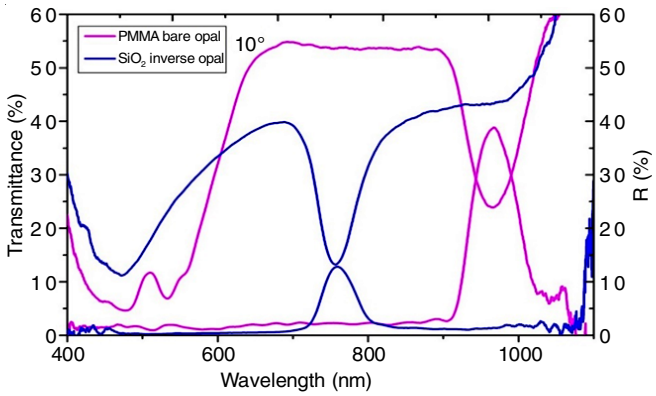

Fig. 3. Graph of optic spectrum for PMMA opal and inverse opal structure with silica

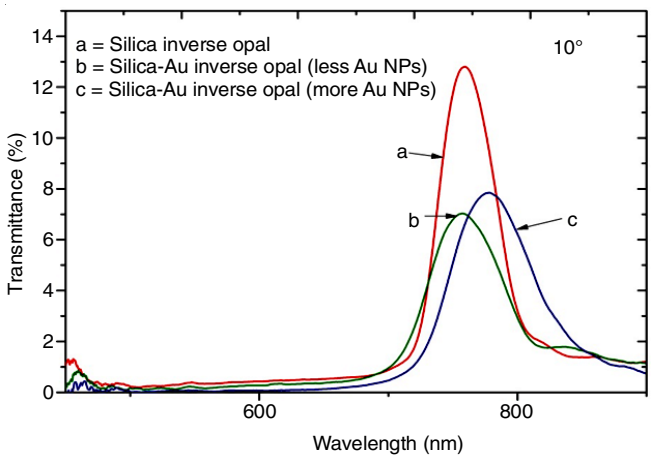

Fig. 4. Transmission spectra of inverted thin film and inverted MPDC thin film with two difference gold nanoparticles percentage incorporated

bare opal and the inverted structure without metal inclusion was determine where photonic bandgap (PBG) was floated at 964 and 757 nm, respectively. The shift that occurred on inverted structure to the bare opal is found to be 207 nm while the inverted MPDC shows 215 and 185 nm for two difference gold nanoparticles incorporation. The summary of Bragg's peak and wavelength shift value is given in Table-1.

This investigation was continued with calculation of the d spacing (Table-2) and the graph was plotted as shown in Fig. 5. From the calculation, the incorporation of gold nanoparticles results in slight blue shift, which is ~8 nm from inverted structure due to the effect of metal refractive index in spectral region towards the silica skeleton. The inverted MPDC with higher percentage of gold nanoparticles incorporated however shows almost 30 nm red shift for the PBG explaining the increment of *d*-spacing where the mobilization of plasmon resonance from the gold nanoparticles in silica skeleton was interestingly occurred.The incorporation of gold nanoparticles bringing an evolution of PBG developed in silica skeleton. This structure bring the phenomena of interplay between the plasmonic absorption, scattering and the plasmonic coupling as the gold nanoparticles was randomly scattered in the interconnected skeleton. However, more works is needs in order to reavaluate this general statement.

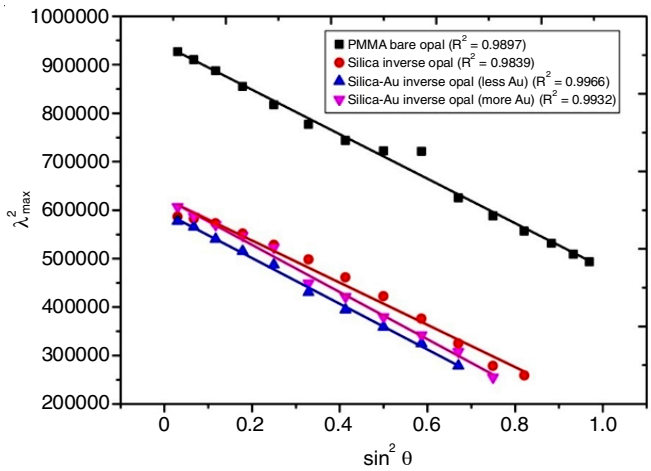

Fig. 5. Graph of λ^2max *versus* $\sin^2\theta$ for PMMA bare opal, inverted structure and inverted MPDC thin film. This data was applied with a degree of departure from the Bragg-Snell's law

Table-2 shows size of particles from SEM measurement and from calculation that was fit on Bragg Snell's equation while lattice d-spacing and refractive index from plotted angle resolved also was calculated. Calculated diameter (D) of PMMA spheres was obtained from eqn 1 shows larger measurement than the diameter obtained from SEM. This is probably due to shrinkage of PMMA spheres under the electron beam.

TABLE-1
WAVELENGTH MAXIMUM VALUE FROM BRAGG PEAK, DIFFERENCE WAVELENGTH FROM BARE OPAL AND INVERSE SiO_2

Samples	λ_{max} measured from Bragg peak ($\theta = 10°$)	$\Delta\lambda$ Change from bare opal	$\Delta\lambda$ Change from inverse SiO_2
PMMA bare opal	964	–	–
Inverted structure	757	207	–
Inverted MPDC (< Au)	749	215	–8
Inverted MPDC (>Au)	779	185	+22

TABLE-2
CALCULATED LATTICE d-SPACINGS, DIAMETERS (D) AND η_{eff} FROM PLOTTED ANGLE-RESOLVED OPTICAL SPECTRA

Samples	d_{111}, Calculated graph plotted (λ^2 *vs.* $\sin^2\theta$) (nm)	D Calculated (nm)	D SEM (nm)	η_{eff} calculated	D calculated from Bragg's peak and η_{eff} value
PMMA bare opal	339	415	373	1.43	415
Inverted structure	356	437	428	1.07	439
Inverted MPDC (less Au)	343	420	470	1.12	414
Inverted MPDC (more Au)	348	427	444	1.13	427

$$d_{111} = D\sqrt{2/3} \quad (1)$$

The plotted graph square of maximum wavelength (λ^2_{max}) against sin 2θ results in linear fit in line with the Bragg-snell's law. According to the plotted graph, the μ_{eff} was found to decrease from PMMA bare opal structure to inverted structure. However the inverted MPDC experiencing slight reduction in μ_{eff} that might due to the existence of gold nanoparticles.

Conclusion

This study was successfully developing a co-crystallization method in order to produce highly performed inverted structure with simple and relatively low cost. The approach of using poly-(methyl methacrylate) (PMMA) as a template in creating inverted photonic crystals introducing great significant as the removal of PMMA require no highly toxic chemical and route. The inverted structure were also upgrade in this study with incorporation of gold nanoparticles in silica skeleton which give rise to PBG peak and enhancing the photonic crystals performance towards photonic and photovoltaic applications. The wide area with crack free film that has been fabricated in this study also behave to be well fitted with Bragg-Snell's equation proving that the resulting material was accepted classified as photonic crystals while produced from a very simple route of production.

ACKNOWLEDGEMENTS

The work was supported by the Science Foundation Ireland for Principal Investigator Grants Numbers 11/PI/117 and 07/IN.1/I787. The support of Fundamental Research Grant Scheme (FRGS) Grants Numbers 59391 is gratefully acknowledged. The support of the School of Fundamental Science, University Malaysia Terengganu and Ministry of Higher Education Malaysia for funding this research are also gratefully acknowledged.

REFERENCES

1. S. Kassim, S.C. Padmanabhan, M. Salaun and M.E. Pemble, *AIP Conf. Proc.*, **1391**, 263 (2011); https://doi.org/10.1063/1.3646852.
2. E. Yablonovitch, *Phys. Rev. Lett.*, **58**, 2059 (1987); https://doi.org/10.1103/PhysRevLett.58.2059.
3. S. John, *Phys. Rev. Lett.*, **58**, 2486 (1987); https://doi.org/10.1103/PhysRevLett.58.2486.
4. C.J.M. Smith, H. Benisty, S. Olivier, M. Rattier, C. Weisbuch, T.F. Krauss, R.M. De La Rue, R. Houdré and U. Oesterle, *Appl. Phys. Lett.*, **77**, 2813 (2000); https://doi.org/10.1063/1.1322367.
5. C. López, *Adv. Mater.*, **15**, 1679 (2003); https://doi.org/10.1002/adma.200300386.
6. P. Jiang, J.F. Bertone, K.S. Hwang and V.L. Colvin, *Chem. Mater.*, **11**, 2132 (1999); https://doi.org/10.1021/cm990080+.
7. A.P. Philipse, *J. Mater. Sci. Lett.*, **8**, 1371 (1989); https://doi.org/10.1007/BF00720190.
8. A. Van Blaaderen, R. Ruel and P. Wiltzius, *Nature*, **385**, 321 (1997); https://doi.org/10.1038/385321a0.
9. R.G. Shimmin, R. Vajtai, R.W. Siegel and P.V. Braun, *Chem. Mater.*, **19**, 2102 (2007); https://doi.org/10.1021/cm0628931.
10. I.M. Povey, D. Whitehead, K. Thomas, M.E. Pemble, M. Bardosova and J. Renard, *Appl. Phys. Lett.*, **89**, 104103 (2006); https://doi.org/10.1063/1.2345359.
11. M. Ibisate, D. Golmayo and C. López, *Adv. Mater.*, **21**, 2899 (2009); https://doi.org/10.1002/adma.200900188.
12. S. Kassim, S. Padmanabhan, J. McGrath and M.E. Pemble, *Appl. Mech. Mater.*, **699**, 318 (2014); https://doi.org/10.4028/www.scientific.net/AMM.699.318.